Journal of Power Sources 223 (2013) 74–78

Contents lists available at SciVerse ScienceDirect

Journal of Power Sources

journal homepage: www.elsevier.com/locate/jpowsour

Short communication

Needle-shaped 3D dye-sensitized solar cells using anodized Ti wire and Pt nanoparticle/carbon fiber electrodes

Mingxuan Sun, Xiaoli Cui*

Department of Materials Science, Fudan University, Shanghai 200433, China

HIGHLIGHTS

- Needle-shaped dye-sensitized solar cells were developed using anodized Ti wire and Pt nanoparticle/carbon fiber.
- Pt nanoparticle/carbon fiber electrode exhibited high catalysis performance toward I_3^-.
- We explored its potential application in parallel connected situation.
- Carbon fiber was first employed as conductive substrate for counter electrode.

GRAPHICAL ABSTRACT

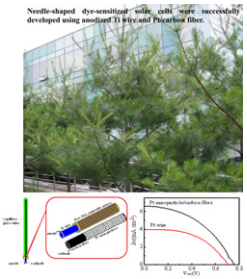

ARTICLE INFO

Article history:
Received 14 June 2012
Received in revised form
31 August 2012
Accepted 3 September 2012
Available online 10 September 2012

Keywords:
Needle-shaped
Dye-sensitized solar cells
Titanium dioxide nanotubes
Platinum nanoparticle
Carbon fiber
Parallel cells

ABSTRACT

Needle-shaped dye-sensitized solar cells are developed using anodized Ti wire and carbon fiber with Pt nanoparticle. The model cell is composed of N719 dye-sensitized TiO_2 nanotubes/Ti wire as working electrode, Pt nanoparticle/carbon fiber as a counter electrode and I^-/I_3^- electrolyte encased in a capillary glass tube with internal diameter of 1.0 mm and 40 mm in length. The as-prepared DSSC looks like a needle leaf of pine tree. The energy conversion efficiency is 2.21% which can be up to 3.07% after $TiCl_4$ post-treatment of photoanodes. In addition, higher current and output power can be obtained by parallel connection. Pt nanoparticle/carbon fiber is firstly used as counter electrode and the cyclic voltammetries investigation show that Pt nanoparticle/carbon fiber possess higher catalytic activity than Pt wire. Such type DSSC is TCO free and may be capable of achieving a long distance transport of photocurrent and harvesting all light from any direction in surroundings to generate electricity. It has been demonstrated that needle-shaped structure may be a good choice for a solar cell.

© 2012 Elsevier B.V. All rights reserved.

1. Introduction

Dye-sensitized solar cells (DSSCs) have been attracting extensive interest in scientific and industrial fields because of low manufacturing costs and high conversion efficiencies. [1] A conventional DSSC is usually based on a planar rigid fluorine-doped tin oxide (FTO) glass substrate with high costs and resistance, which is not suitable for transportation, installation, and remote application. In addition, the planar cell structure is a limitation for the full potential absorption of solar light. Moreover, the Pt counter electrode (CE) is an expensive noble metal, which can become a heavy burden for further development of DSSCs. All of these prevent the development of the large-scale industrial manufacturing of the DSSC. Until now, a variety of DSSCs have been designed to meet requirements, including the application of metal or carbonous substrates in DSSCs [2,3], three-dimensional (3D) DSSCs, [4–6] wire-shaped DSSCs, [7–10] and low Pt loading [11] or non-platinum DSSCs [12–14].

Many research efforts have been focused on the replacement of FTO glass with metal or carbonous substrate due to its good conductivity, low cost and high temperature endurance compared

* Corresponding author. Tel./fax: 86 21 65642397.
E-mail address: xiaolicui@fudan.edu.cn (X. Cui).

0378-7753/$ – see front matter © 2012 Elsevier B.V. All rights reserved.
http://dx.doi.org/10.1016/j.jpowsour.2012.09.009

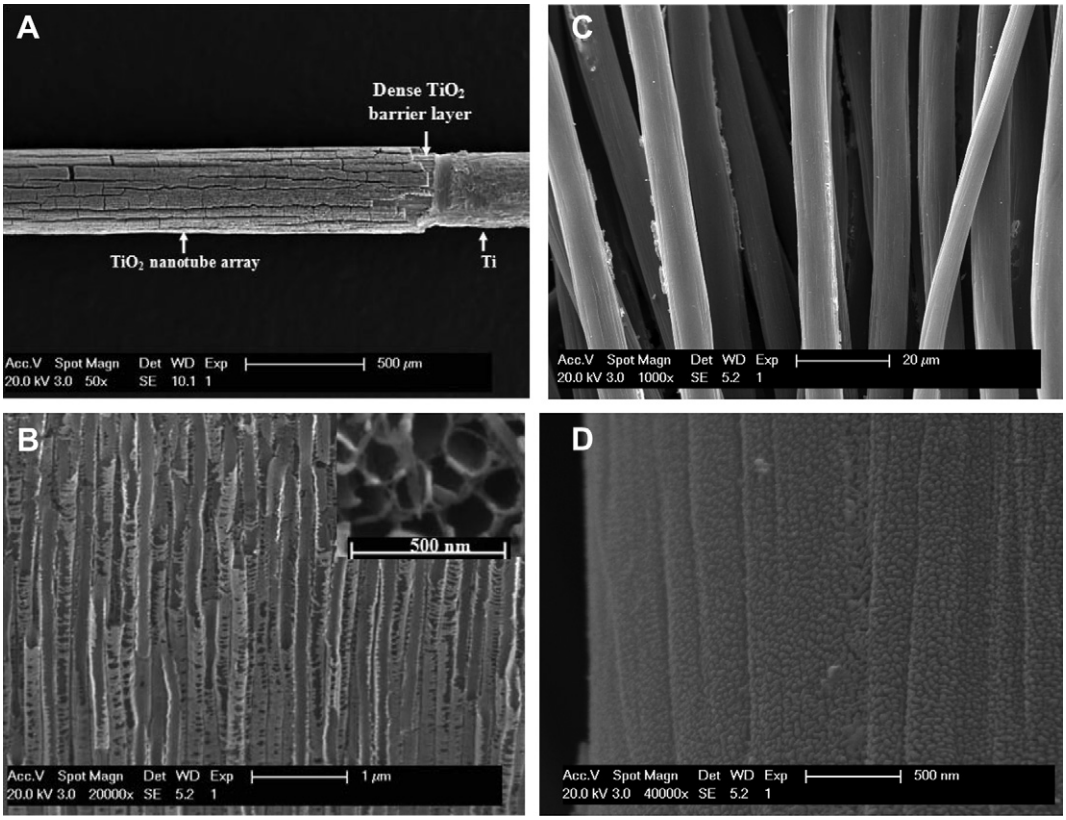

Fig. 1. FE-SEM characterization. (A) FE-SEM images of the photoanode with two parts, including an inner Ti core and anodically grown TiO_2 nanotube arrays. (B) Cross-section FE-SEM image of TiO_2 nanotube arrays grown around a Ti wire; the inset is the top morphology of TiO_2 nanotube arrays. (C) and (D) FE-SEM images of Pt nanoparticle/carbon fiber.

with the FTO substrate. Zou et al. [2] fabricated the first generation of all-metal DSSC by using stainless steel mesh as the substrate and coated it with dense and porous TiO_2 layers. The conversion efficiency is about 1.49%. Guo et al. [3] reported rectangular bunched rutile TiO_2 nanorod arrays grown on carbon fiber was used successfully as photoanode in DSSC and energy conversion efficiency of 1.28% was achieved. Carbon fibers are flexible, conductive and stable in liquid electrolyte. They also have large surface area and good heat resistance and fatigue. Thus, they could be promising candidates for conductive substrates in DSSCs.

The counter electrode affects the performance of the DSSCs by modifying the electrical conductivity and the catalytic activity for the regeneration of the I_3^-/I^- species. Platinum is the most superior counter electrode material with excellent catalytic activity and high electrical conductivity. However, the high price of Pt undoubtedly limits its application for large-scale production of DSSCs. Therefore, many research efforts have been focused on exploiting inexpensive substitutes for Pt, such as carbon materials [15,16], conductive organic polymers [17,18], and inorganic materials [19]. In addition, reducing the loading amount of Pt is another alternative method to reduce the costs [11].

Titania has been proved to be one of the most promising candidates for photoanodes until now [20–24]. The use of TiO_2 nanotubes in conventional planar DSSCs can effectively improve the charge collection efficiency [25–28]. Very recently, using TiO_2 nanotube arrays on Ti wires have been reported [4,29,30]. Liu et al. [30] demonstrated a prototype dye-sensitized photovoltaic wire with a conversion efficiency of 2.78% using anodized Ti wire as working electrode and platinum wire as counter electrode. The advantages of Ti wire have been realized but there is great challenge to enhance its conversion efficiency and to decrease its cost by exploiting inexpensive substitutes for Pt wire.

3D DSSCs exhibit superiority of absorbing sun light from all directions. Wang et al. [4] fabricated a 3D DNA-like structure dye-sensitized solar cell with all-Ti substrates, which showed superiority of light utilization due to its symmetrical double-helix structure. Weintraub et al. [5] demonstrated an optical fiber/nanowire hybrid structures for efficient 3D three-dimensional dye-sensitized solar cells. The optical fiber is used as a channel of the light incident and the internal reflection of the light within it creates multiple opportunities for energy conversion.

In the nature, many kinds of plant leaves have been evolved to capture the solar energy more effectively. For example, the needle leaves of pine tree grown around the stem in orderly screw pattern can avoid shading each other and is not sensitive to the sun azimuth. Inspired by the needle leaves of pine tree, we fabricated a needle-shaped 3D structure of DSSCs in this work. The conversion efficiency is 3.07% using highly ordered TiO_2 nanotube arrays radically grown around a Ti wire post treated by $TiCl_4$ and Pt nanoparticle/carbon fiber as the counter electrode. The Ti metal wire and carbon fiber played a key role in reducing the internal resistance of DSSCs. As far as we are aware, this is the first time that carbon fiber is used as the counter electrode substrate. In addition, the cells in parallel were also achieved for the first time. It has been demonstrated that needle-shaped structure may be a good design for a solar cell.

2. Experimental section

2.1. Fabrication of the photoanode

The titanium wires (0.4 mm) were chemically etched by dipping in an HF (40%)–HNO_3 (65%)–H_2O (1:4:5 in volume) solution for 20 s. The etched wires were repeatedly rinsed in deionized water

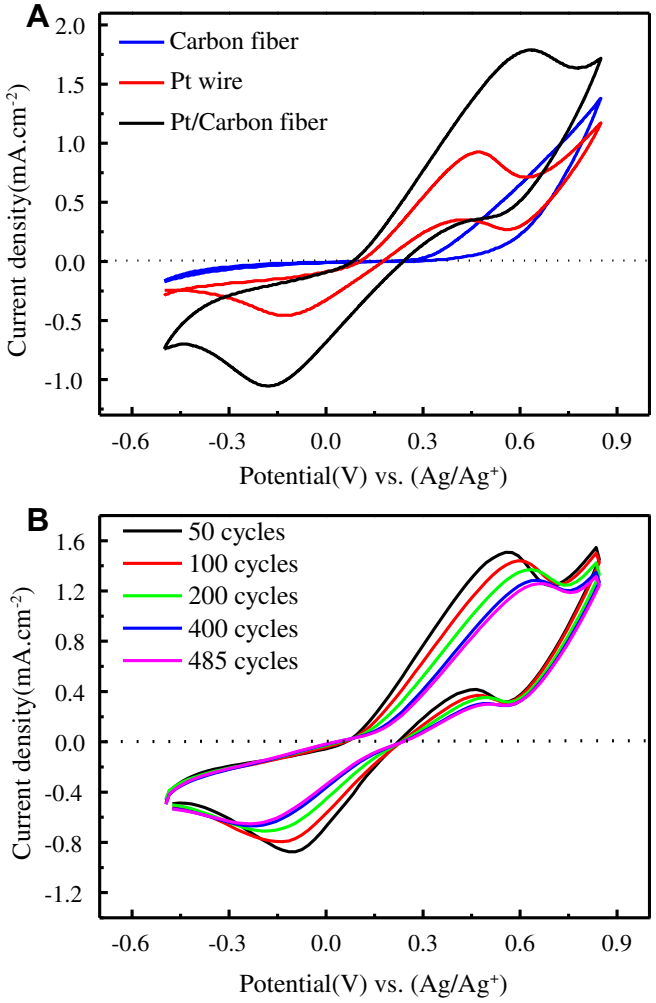

Fig. 2. Cyclic voltammograms of triiodide/iodide redox couple for Pt nanoparticle/carbon fiber electrodes. (A) The comparison of carbon fiber electrodes and Pt nanoparticle/carbon fiber electrodes at the scan rate of 50 mV s^{-1}. (B) The stability test of Pt nanoparticle/carbon fiber electrodes.

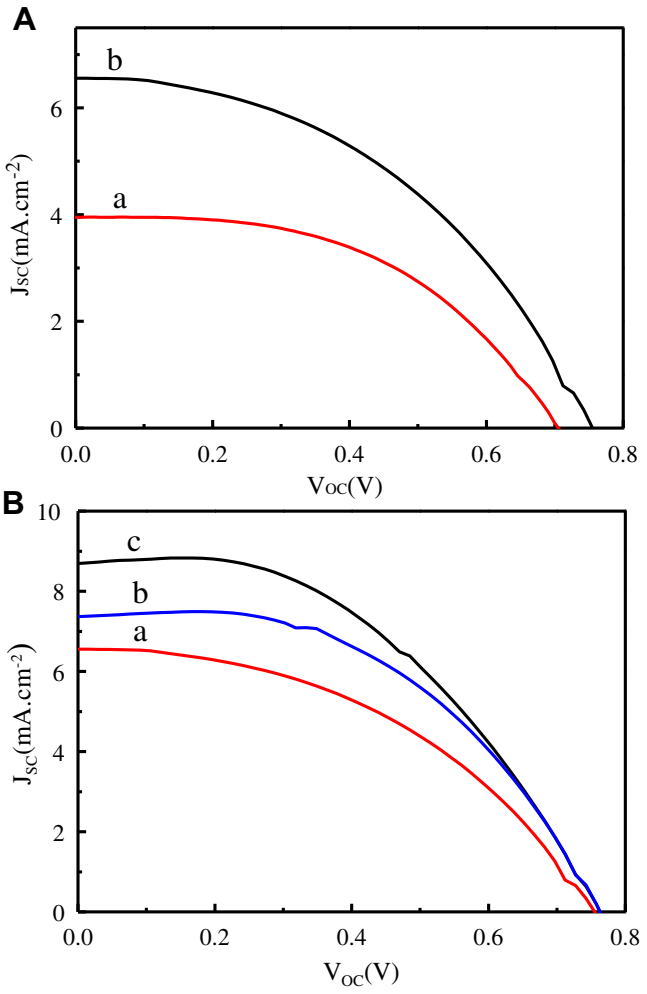

Fig. 3. Photocurrent density–photovoltage (J–V) curves for DSSCs. A: The comparison of photovoltage performance based on Pt (a) and Pt nanoparticle/carbon fiber (b). B: The effect of $TiCl_4$ post treatment. a. TiO_2 nanotubes. b. TiO_2 nanotubes post-treated by $TiCl_4$ for 1 h at room temperature. c. TiO_2 nanotubes post-treated by $TiCl_4$ for 1 h at 60 °C.

followed by drying in an air stream and used immediately. The polished Ti wire was anodized in ethylene glycol solution containing 0.6 wt% NH_4F and 3.5 v% H_2O for 1 h at 60 V using a DC power supply. Finally, the as-prepared samples were rinsed in deionized water and then sintered at 450 °C for 2 h in atmospheric air. Prior to dye adsorption, the annealed samples were immersed in 0.2 M $TiCl_4$ for 1 h at 60 °C (or at room temperature) and then fully rinsed with ethanol and sintered at 450 °C for 30 min. After cooling down to 80 °C, the TiO_2 nanotubes were dipped in a dye solution of 5×10^{-4} M N719 dissolved in absolute ethanol and kept at room temperature for 12 h in order to obtain the dye-sensitized TiO_2 nanotube photoanode.

2.2. Fabrication of the counter electrode

The carbon fiber (0.4 mm) was first rinsed in water, ethanol and acetone ultrasonically for 5 min and then kept immersed in a 10 mM H_2PtCl_6 ethanol solution overnight. After that, it was thermally treated at 385 °C for 20 min. Thus, the carbon fiber supported Pt nanoparticle (Pt/carbon fiber) was prepared by a thermal decomposition process. Full electrochemical measurements were performed for this electrode.

2.3. Assembly of DSSCs

The dye-sensitized photoanode and Pt nanoparticle/carbon fiber were put into transparent glass tube (internal diameter 1.0 mm) in parallel and sealed by silicone rubber. The redox electrolyte composed of 0.05 M I_2, 0.1 M LiI, 0.1 M guanidinium thiocyanate, 0.1 M N-methylbenzimidazole and 0.5 M 4-tert-butylpyridine in 3-methoxypropionitrile was injected into it by syringe. In order to preliminarily explore its potential application in large area, we fabricated the parallel connected DSSCs with two and three cell units.

2.4. Measurements and characterization

Surface morphology and cross-sectional images were studied by field emission scanning electron microscopy (FE-SEM, Philips XL30). The electrochemical measurements were performed on a CHI 660 electrochemical workstation (Shanghai Chenhua Instruments, China) in a three-electrode system, with Pt nanoparticle/carbon fiber, Pt foil and Ag/AgCl as the working electrode, counter electrode and reference electrode, respectively. Cyclic voltammograms (CV) were recorded in 10 M LiI + 1 M I_2 + 0.1 M $LiClO_4$ acetonitrile solution with the potential range from −0.5 to 0.85 V.

Table 1
The comparison of photovoltaic performance of the as-fabricated DSSCs. DSSCs based on Pt (a) and Pt nanoparticle/carbon fiber (b). DSSCs based on TiO_2 nanotube post-treated by $TiCl_4$ at room temperature (c) and 60 °C (d) for 1 h.

	J_{SC}(mA cm^{-2})	V_{OC}(V)	*FF*	Efficiency (%)
A	3.94	0.71	0.50	1.40
B	6.43	0.75	0.46	2.21
C	7.35	0.76	0.50	2.81
D	8.67	0.76	0.47	3.07

The performance of the dye-sensitized solar cells (DSSCs) was tested by recording the current density voltage (J–V) curves with a Keithley 2420 source meter under illumination of simulated AM 1.5 solar light from a solar simulator (roel sol3A class AAA solar simulator, model 94023A and an AM 1.5 filter).

3. Results and discussion

The morphology of resulted TiO_2 nanotubes and Pt nanoparticle/carbon fiber were characterized by field emission scanning electron microscopy (FE-SEM) images. As shown in Fig. 1A, the anodized Ti wire has three parts, including Ti core wire, dense TiO_2 barrier layer and TiO_2 nanotube arrays. TiO_2 nanotube arrays are vertical to Ti substrate, which provide unidirectional channels for the charge transport. The length of TiO_2 nanotubes can be controlled by altering the anodization duration and voltage. Furthermore, a dense TiO_2 barrier layer forms at the interfaces of Ti metal and TiO_2 nanotubes when the sample is anodized and further annealed. It is able to effectively block the back electron transfer from the substrate to the electrolyte, which is considered to be quite vital to suppress the generation of dark current in the DSSCs. The typical cross sectional and top view SEM images of the TiO_2 nanotubes are presented in Fig. 1B and inset. The TiO_2 nanotube arrays are well-defined with a single tube internal diameter of approximately 149 nm and a wall thickness of about 21 nm. Fig. 1C and D present the morphology of Pt nanoparticle/carbon fiber. It can be seen that a layer of Pt nanoparticle with diameters in the range of 21–43 nm were dispersed on the surface of carbon fiber, which demonstrates the successful fabrication of carbon fiber supported Pt nanoparticle counter electrode. Moreover, a large surface area of the Pt nanoparticle layer could be observed. Thus, we expect a high catalysis performance when it is used in dye-sensitized solar cells.

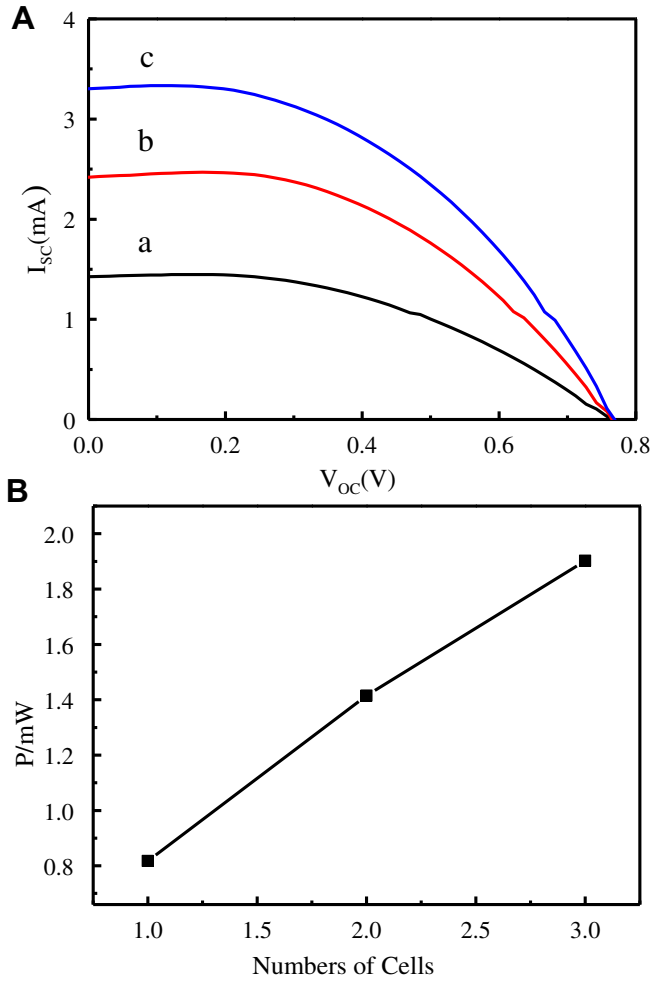

Fig. 4. Photocurrent–photovoltage (I–V) curves for parallel DSSCs (A) and the comparison of output power for cells in parallel (B). a. one cell b. two cells c. three cells.

Table 2
Comparison of photovoltaic properties of parallel cells.

	J_{SC}(mA cm^{-2})	I_{SC}(mA)	V_{OC}(V)	*FF*	Efficiency (%)	Power (mW)
One cell	8.67	1.4	0.76	0.47	3.07	0.8
Two cells	7.46	2.4	0.76	0.48	2.74	1.4
Three cells	6.73	3.3	0.77	0.47	2.41	1.9

To evaluate the electrocatalytic activity of the Pt nanoparticle/carbon fiber toward the reduction of I_3^-, cyclic voltammetry measurements were carried out in a three-electrode system. Fig. 2 displays the cyclic voltammograms of the I_3^-/I^- redox couple on Pt nanoparticle/carbon fiber counter electrode under dark condition. There are obvious redox waves for the Pt nanoparticle/carbon fiber compared with carbon fiber counter electrode in Fig. 2A. The relative peak in negative potential corresponds to a reduction of I_3^- ions [31,32]. In cyclic voltammetry, peak area and current density for reaction usually increases with the increase in the reaction rate [33,34]. It can be seen that the redox peak current density of I_3^-/I^- at the Pt nanoparticle/carbon fiber electrode is obvious, indicating a quick redox reaction at Pt nanoparticle/carbon fiber electrode, while the redox peaks for Pt wire is smaller than Pt nanoparticle/carbon fiber CE. Moreover, no obvious redox peaks were observed for carbon fiber. Herein, we can deduce that Pt nanoparticle/carbon fiber is more effective than Pt in catalyzing the triiodide reduction, whereas carbon fiber is as effective as FTO at collecting and transporting electrons. Therefore, Pt nanoparticle/carbon fiber can be used successfully to replace the expensive Pt wire in DSSCs.

Moreover, the stability of the as-prepared Pt nanoparticle/carbon fiber was also detected. Fig. 2B shows the typical cyclic voltammogram (CV) as a function of the number of cycles. As the number of cycles increases, the cathodic current density peak decreases slightly. The steady state of the cathodic current peak after about 485 cycles is attributed to the catalytic stability of the as-prepared electrode.

Fig. 3 shows the photocurrent density–photovoltage (J–V) characteristics of the DSSCs fabricated with TiO_2 nanotubes and Pt nanoparticle/carbon fiber. The detailed photovoltaic parameters are listed in Table 1. The DSSC with Pt nanoparticle/carbon fiber achieved a power conversion efficiency of 2.21%, which was 1.57 times of that using Pt counter electrode (1.40%) (Fig. 3A). In addition, the Pt nanoparticle/carbon fiber yielded a relatively high short circuit current. The results are related to the high catalytic activity of Pt nanoparticle/carbon fiber which maybe attributed to its higher surface area. It can be used as a promising counter electrode catalyst. This is also in conformity with the CV results.

Fig. 3B shows the effects of $TiCl_4$ post-treatment on the J–V characteristics of dye-sensitized TiO_2 nanotube solar cells. The $TiCl_4$ treatment of the TiO_2 nanotubes at room temperature has resulted in

an increase in short-circuit photocurrent (Jsc) from 6.43 mA cm^{-2} to 7.35 mA cm^{-2} for the DSSC and increase in energy conversion efficiency (η) from 2.21% to 2.81%. For $TiCl_4$-treated nanotube array at 60 °C, the relative DSSCs exhibited J_{sc} of 8.64 mA cm^{-2}, and conversion efficiency of 3.07%. We note that this efficiency is 1.4 times the efficiency of non-$TiCl_4$-treated nanotubes. The three modules of DSSCs exhibited similar open circuit voltage (Voc) values and fill factor (FF) with variations in short circuit current density (Jsc). $TiCl_4$ post-treatment for the TiO_2 nanotubes is effective in increasing photocurrent. We hypothesize that the $TiCl_4$ treatment facilitates improved bonding between the TiO_2 and dye molecule, resulting in improved charge transfer and decreased surface recombination [35–37].

Fig. 4 illustrates the photocurrent–voltage (I–V) characteristic performances of single cell and the parallel connected DSSCs. The detailed photovoltaic parameters are listed in Table 2. As shown in Fig. 4A, the one cell achieved an open voltage of 0.76 V, a short circuit current of 1.42 mA and a conversion efficiency of 3.07%. On the other hand, the parallel connected DSSCs with two cell units had an open voltage of 0.76 V, a short circuit current of 2.42 mA and a photoelectric efficiency of 2.74%. Upon further investigation, an open voltage of 0.77 V, a short circuit current of 3.29 mA and a photoelectric conversion efficiency of approximately 2.41% were achieved for cells composed of three DSSCs units in parallel. The short circuit current has increased with the number of parallel connected DSSCs, whereas the photovoltage has remained the same, which resulted in the increase of output power (Fig. 4B). The advantage of the parallel connection becomes evident when comparing I–V characteristics of the whole DSSC with those of the single compartments individually. It is expected to obtain a higher energy conversion efficiency if the optimum number of cells are connected in parallel.

4. Conclusions

In summary, novel needle-shaped DSSCs have been developed by using highly ordered TiO_2 nanotube arrays radically grown around Ti wire photoanode and Pt nanoparticle/carbon fibers counter electrode. Pt nanoparticle/carbon fibers exhibited an impressive catalytic activity on the reduction of triiodide. The DSSC based on Pt nanoparticle/carbon fibers reached an energy conversion efficiency of 2.21%, which is higher than that of the DSSC using Pt wire (1.40%). Photoanodes treated with titanium tetrachloride solution are found to be effective for improving the photocurrent densities of the needle shaped solar cells. The present work reports for the first time the use of conductive carbon fiber as a conductive substrate for counter electrode of DSSCs. The results demonstrated that Pt nanoparticle/carbon fiber is a promising alternative to the noble metal Pt wire in the application of DSSCs. In addition, this novel DSSC is capable of harvesting the light incident from any direction.

Acknowledgements

This work was supported by the Natural Science Foundation of China (No 21273047) and the National Basic Research Program of China (No. 2012CB934300, 2011CB933300). The authors would also like to thank Professor Ming Lu (Department of Optics Science and Engineering, Fudan University) for the assistance in the measurements of I–V curves. We also appreciate the referee's very valuable comments, which have greatly improved the quality of the manuscript.

References

[1] A. Yella, H.W. Lee, H.N. Tsao, C. Yi, A.K. Chandiran, M.K. Nazeeruddin, E.W.G. Diau, C.Y. Yeh, S.M. Zakeeruddin, M. Grätzel, Science 334 (2011) 629–634.
[2] X. Fan, F. Wang, Z. Chu, L. Chen, C. Zhang, D. Zou, Appl. Phys. Lett. 90 (2007) 073501–073503.
[3] W.X. Guo, C. Xu, X. Wang, S.H. Wang, C.F. Pan, C.J. Lin, Z.L. Wang, J. Am. Chem. Soc. 134 (2012) 4437–4441.
[4] Y.H. Wang, Y. Liu, H.X. Yang, H. Wang, H. Shen, M. Li, J. Yan, Curr. Appl. Phys. 10 (2010) 119–123.
[5] B. Weintraub, Y.G. Wei, Z.L. Wang, Angew. Chem. Int. Ed. 48 (2009) 1–6.
[6] Y. Liu, H. Wang, H. Shen, W. Chen, Appl. Energy 87 (2010) 436–441.
[7] X. Fan, Z.Z. Chu, F.Z. Wang, C. Zhang, L. Chen, Y. Chen, Y.W. Tang, D.C. Zou, Adv. Mater. 20 (2008) 592–595.
[8] M.R. Lee, R.D. Eckert, K. Forberich, G. Dennler, C.J. Brabec, R.A. Gaudiana, Science 324 (2009) 232–235.
[9] D.C. Zou, D. Wang, Z.Z. Chu, Z.B. Lv, X. Fan, Coord. Chem. Rev. 254 (2010) 1169–1178.
[10] D. Wang, S.C. Hou, H.W. Wu, C. Zhang, Z.Z. Chu, D.C. Zou, J. Mater. Chem. 21 (2011) 6383–6388.
[11] K.C. Huang, Y.C. Wang, R.X. Dong, W.C. Tsai, K.W. Tsai, C.C. Wang, Y.H. Chen, R. Vittal, J.J. Lin, K.C. Ho, J. Mater. Chem. 20 (2010) 4067–4073.
[12] M.X. Wu, X. Lin, A. Hagfeldt, T.L. Ma, Angew. Chem. Int. Ed. 50 (2011) 3520–3524.
[13] M.X. Wu, X. Lin, A. Hagfeldt, T.L. Ma, Chem. Commun. 47 (2011) 4535–4537.
[14] Y.D. Wang, M.X. Wu, X. Lin, Z.C. Shi, A. Hagfeldt, T.L. Ma, J. Mater. Chem. 22 (2012) 4009–4014.
[15] H. Choi, H. Kim, S. Hwang, Y. Han, M. Jeon, J. Mater. Chem. 21 (2011) 7548–7551.
[16] G. Zhu, L.K. Pan, T. Lu, T. Xu, Z. Sun, J. Mater. Chem. 21 (2011) 14869–14875.
[17] H.C. Sun, Y.H. Luo, Y.D. Zhang, D.M. Li, Z.X. Yu, K.X. Li, Q.B. Meng, J. Phys. Chem. C 114 (2010) 11673–11679.
[18] S. Ameen, M.S. Akhtar, Y.S. Kim, O.B. Yang, H.S. Shin, J. Phys. Chem. C 114 (2010) 4760–4764.
[19] J. Li, M.X. Sun, X.Y. Zhang, X.L. Cui, Acta Phys-Chim. Sin. 27 (2011) 2255–2268.
[20] M.X. Sun, X.Y. Zhang, J. Li, X.L. Cui, D.L. Sun, Y.H. Lin, Electrochem. Commun. 16 (2012) 26–29.
[21] M.X. Sun, X.L. Cui, Electrochem. Commun. 20 (2012) 133–136.
[22] P. Song, X.Y. Zhang, M.X. Sun, X.L. Cui, Y.H. Lin, Nanoscale 4 (2012) 1800–1804.
[23] C.R. Ke, J.M. Ting, J. Power Sources 208 (2012) 316–321.
[24] W.K. Tu, C.J. Lin, A. Chatterjee, G.H. Shiau, S.H. Chien, J. Power Sources 203 (2012) 297–301.
[25] P. Roy, D. Kim, K. Lee, E. Spiecker, P. Schmuki, Nanoscale 2 (2010) 45–59.
[26] B.X. Lei, J.Y. Liao, R. Zhang, J. Wang, C.Y. Su, D.B. Kuang, J. Phys. Chem. C 114 (2010) 15228–15233.
[27] P. Zhong, W.X. Que, J. Chen, X. Hu, J. Power Sources 210 (2012) 38–41.
[28] R. Liu, W.D. Yang, L.S. Qiang, J. Power Sources 199 (2012) 418–425.
[29] S. Zhang, C.Y. Ji, Z.Q. Bian, R.H. Liu, X.Y. Xia, D.Q. Yun, L.H. Zhang, C.H. Huang, A.Y. Cao, Nano Lett. 11 (2011) 3383–3387.
[30] Z.Y. Liu, M. Misra, ACS Nano 4 (2010) 2196–2200.
[31] B. Zhao, H. Huang, P. Jiang, H. Zhao, X. Huang, P. Shen, D. Wu, R. Fu, S. Tan, J. Phys. Chem. C 115 (2011) 22615–22621.
[32] R. Bajpai, S. Roy, N. Kulshrestha, J. Rafiee, N. Koratkar, D.S. Misra, Naoscale 4 (2012) 926–930.
[33] Z. Huang, X.Z. Liu, K.X. Li, D.M. Li, Y.H. Luo, H. Li, W.B. Song, L.Q. Chen, Q.B. Meng, Electrochem. Commun. 9 (2007) 596–598.
[34] M.X. Wu, X. Lin, T.H. Wang, J.H. Qiu, T.L. Ma, Energy Environ. Sci. 4 (2011) 2308–2315.
[35] J. Wang, Z.Q. Lin, Chem. Mater. 22 (2010) 579–584.
[36] B. Liu, E.S. Aydil, J. Am. Chem. Soc. 131 (2009) 3985–3990.
[37] N. Huang, Y. Liu, T. Peng, X. Sun, B. Sebo, Q. Tai, H. Hu, B. Chen, S. Guo, X. Zhao, J. Power Sources 204 (2012) 257–264.